

Studies on Chemical Resistance of PET-Mortar Composites: Microstructure and Phase Composition Changes

Ahmed Soufiane Benosman^{1,2,3*}, Mohamed Mouli², Hamed Taibi¹, Mohamed Belbachir¹,
Yassine Senhadji², Ilies Bahlouli¹, David Houivet⁴

¹Faculty of Science, Laboratory of Polymer Chemistry, University of Oran, Es-Senia, Algeria

²Department of Civil Engineering, Laboratory of Materials, ENSET, Oran, Algeria

³Department of Chemistry, Preparatory School of Science and Technology EPST, Tlemcen, Algeria

⁴University of Caen Basse-Normandie, Laboratory of LUSAC EA 2607, Cherbourg Octeville, France

Email: *amre20022000@yahoo.fr

Received January 10, 2013; revised February 11, 2013; accepted February 18, 2013

Copyright © 2013 Ahmed Soufiane Benosman *et al.* This is an open access article distributed under the Creative Commons Attribution License, which permits unrestricted use, distribution, and reproduction in any medium, provided the original work is properly cited.

ABSTRACT

Researches into new and innovative uses of waste plastic materials are continuously advancing. These research efforts try to match society's need for safe and economic disposal of waste materials. The use of recycled plastic aggregates saves natural resources and dumping spaces, and helps to maintain a clean environment. The present articles deals with the resistance to chemical attack of polymer-mortars, which are often used as low-cost promising materials for preventing or repairing various reinforced concrete structures. To gain more knowledge on the efficiency of polymer-mortar composites, four mortar mixtures: one specimen with Portland cement and three mixtures with 2.5, 5, and 7.5 wt% of the substitution of cement by polyethylene terephthalate (PET) were exposed to the influence of aggressive environment (0.5%, 1% and 1.5% HCl acids, 10% NH₄Cl, 5% H₂SO₄ acid and 10% (NH₄)₂SO₄ solutions). The measurements of several properties were carried out, the results were analyzed and the combination of X-ray diffraction, FT-IR spectroscopy, differential thermal analysis (DTA), thermogravimetric (TG) analysis, differential scanning calorimetry (DSC) analysis and the composites were also observed by SEM led to the positive identification of the deterioration products' formation. From this study, it was found that the addition of PET to the modified mortars, means reducing the penetration of aggressive agents. So, the PET-modified mortars exposed to aggressive environments showed better resistance to chemical attack. The new composites appear to offer an attractive low-cost material with consistent properties. The present study highlights the capabilities of the different methods for the analysis of composites and opened new way for the recycling of PET in polymer-mortars.

Keywords: Composite; Polymer-Mortar; PET Waste; Acids; NH₄Cl Attack; Ammonium-Sulfate Attack; Microstructure

1. Introduction

Degradation of concrete, as well as the related protection and ensuring of concrete structures against aggressive impacts by chemical agents, regardless of whether this concerns liquid, gas, or even solid phase under certain conditions, represents a complex problem of utmost importance for the economy in general, and especially for building construction and the construction industry [1]. Therefore, polymer-modified mortars have been popular

construction materials because of their excellent properties in comparison with ordinary mortars. Polymers have been used for improving mechanical properties, adhesion with substrates, or waterproofing properties of mortars and concretes. The literature agrees that the properties of polymer modified mortar and concrete depend significantly on the polymer content or polymer-cement ratio, that is, the mass ratio of the amount of polymer solids in a polymer-based admixture to the amount of cement in a polymer-modified mortar or concrete [2-4].

A substantial growth in the consumption of plastic is

*Corresponding author.

observed all over the world in recent years, which has led to huge quantities of plastic-related waste. Recycling of plastic waste to produce new materials like concrete, mortar or composite appears as one of the best solution for disposing of plastic waste, due to its economic and ecological advantages. Several works have been performed or are under way to evaluate the properties of cement-composites containing various types of plastic waste as aggregate, filler or fibre [5,6].

Depending on the appropriate final target, varied types of waste can be used in concrete: Portella *et al.* [7] and Guerra *et al.* [8] have studied the properties of concrete with addition of ceramic waste; Ismail and Al-Hashmi [9] have studied concrete with recycled plastic addition; Angulo *et al.* [10] have characterized recycled materials from construction and demolition as an aggregate for concrete; and, amongst others, Hoppen *et al.* [11] have found in concrete the possibility to deposit the residual sludge from water treatment stations.

Different works, as of Rebeiz [12], Choi *et al.* [13,14] and JO *et al.* [15], have analyzed the effect of addition of recycled PET to the properties of concrete. The fibers of recycled PET easily mix in the concrete, giving new properties to the material [16]. Khaloo *et al.* [17] have observed that the addition of tire rubber particles provided the concrete with higher ductility in compressive strength testing, if compared with concrete without addition. J. C. A. Galvão *et al.* [18] have demonstrated a better performance to use of waste polymers (PET, LDPE and rubber from useless tires) in concrete for repair of dam hydraulic surfaces. Wang *et al.* [19] have analyzed a Performance of cement mortar made with recycled high impact polystyrene, which is a common component of consumer electronics. Corinaldesi *et al.* [20] have also showed a better mechanical behaviour and thermal conductivity of mortars containing waste rubber particles coming from wasted rubber-shoe outsoles (SR, acronym of "sole rubber"). In the previous work [21,22], the author studied the effects of PET polymer on the mortar properties, specifically to decrease the chloride ion penetration depth and apparent chloride ion diffusion coefficient of polymer-mortar composites. This may be explained due to the reduced volume of large-sized pores and the improved resistance to the absorption of the test solutions with an increase in polymer-cement ratio [22]. In addition, Gouasmi *et al.* [23,24] showed the improvement of the adherence strength and the resistance to aggressive solutions of composites using waste PET lightweight aggregates (WPLA). One of the advantages of the use of recycled plastic in concrete is the reduction of solid waste in landfills [5,6].

Polyethylene terephthalate (PET) is one of the most common consumer plastics used and is widely employed as a raw material to realize products such as blown bot-

tles for soft-drink use and containers for the packaging of food and other consumer goods. PET bottles have taken the place of glass bottles as storing vessel of beverage due to its lightweight and easiness of handling and storage.

In 2007, it is reported a world's annual consumption of PET drink covers of approximately 10 million tons, which presents perhaps 250 milliards bottles. This number grows about up to 15% every year [25]. On the other hand, the number of recycled or returned bottles is very low. Generally, the empty PET packaging is discarded by the consumer after use and becomes PET waste (WPET). The major problems that this level of waste production generates initially entail storage and elimination [26]. The recycling of PET bottles and the preservation of natural resources are priority items but to date, the recycling of PET bottles as a lightweight aggregate for concrete has not been studied because of the high melting cost [16].

Chemical degradation of concrete is the consequence of reactions between the constituents of cement stone, *i.e.*, calcium silicates, calcium aluminates, and above all calcium hydroxide, as well as other constituents, with certain substances from water, solutions of soil, gases, vapors, acids etc. The most important aggressive agents are: SO_4^{2-} , Mg^{2+} , NH_4^+ , Cl^- , H^+ , and HCO_3^- [1,27,28].

When speak about sulfate degradation, we primarily think of the impact by sulfate ions on cement stone. The sulfate ion is the cause of one of the most dangerous corruptions—the corrosion of expansion and swelling—because it causes the occurrence of expansive compounds, the most important of which is ettringite, $\text{C}_3\text{A}\cdot 3\text{CaSO}_4\cdot 32\text{H}_2\text{O}$, in the shape of prismatic crystals [29,30].

For the process of concrete degradation under the impact of sulfates, it is essential which cation is linked with the sulfate ion. Namely, cations linked with sulfate ions can be divided into three characteristic groups [1]. The first group includes alkali metals Na^+ and K^+ , which give extremely soluble hydroxides, while the second group comprises metals such as Mg^{2+} and Fe^{2+} , which give poorly soluble hydroxides, and the third group consists of cations NH_4^+ and H^+ , which give volatiles or hydroxide. The third group of sulfates, that is $(\text{NH}_4)_2\text{SO}_4$ and H_2SO_4 , covers the most aggressive compounds. In case of impact by these compounds on concrete, there occurs not only expansion, but also intensive dissolution of cement stone [1].

The degree of aggressivity of an acid is dependent on the chemical character of anions present. The strength of acid, its dissociation degree in solutions and, mainly, the solubility of the salt formed are dependent on the chemical character of anion. With respect to concrete acidic attack, the solubility of calcium salts formed is of a great

significance. Because the acidic attack is based on the processes of decomposition and leaching of the constituents of cement matrix, the conditions of transport phenomena, such as the supply of aggressive acidic solutions and draining of the products of the attack is of specific significance for the intensity of attack [31-33].

In addition, a parameter which is tightly connected with the properties of acids is that their pH reaches a value of approximately 5 and lower. The severity of the acidic attack is significantly dependent on the solubility of the calcium salt formed. In the case of the formation of highly soluble salts, the severity of the attack is very high. This is caused by the dissolving and leaching of the formed salt from the attacked material. A very porous layer of corrosive products remains on the surface, contributing to further development of the deterioration process. In the case of the formation of insoluble calcium salts such as calcium oxalate and sulfate the effect of the acidic solution is entirely different. A dense insoluble layer is formed enhancing the development of the acidic attack showing a protective effect. This is used in practice for the protective purposes [34].

The objective of the research reported here was to evaluate the chemical resistance of polymer-mortar composites containing a waste polyethylene terephthalate PET, as a substitute of the cement used in the mix, under hydrochloric acid, ammonium-chloride, ammonium-sulfate and sulfuric acid solutions exposure. The identification of the deterioration products' which appear on the surface of the samples were analyzed by X-ray diffraction, FTIR, SEM, ATD, TG/dTG and DSC analyses. However, no pertinent data were previously found concerning the effect of PET against ammonium-chloride or ammonium-sulfate attack. So, in this paper the durability of PET-mortar composites exposed to aggressive solutions has been investigated. If successful, such an application of waste PET, as substitute of cement, will be a major step towards reducing the solid waste disposal problem and reliance on natural resources, thereby reducing environmental pollution and energy consumption. Additionally, the immediate consequence is the anticipated necessity of maintenance and repairs of the concrete structures, which must have specific characteristics, mainly mechanical and chemical, based on the material of the base or its substratum.

2. Materials, Experimental Design and Methods

2.1. Raw Materials

The cement used was a blended Portland cement type CPJ-CEM II/A (pouzzolanic cement) delivered from Zahana factory located in the western Algeria, chemical and physical properties of cement are shown in **Tables 1**

and **2**, respectively, according to the manufactories. The chemical composition was obtained by using an X-ray fluorescence spectrometer analysis type OXFORD MD X¹⁰⁰⁰.

Two different aggregate types were selected for this study, sand (S) and PET particles. Those come from drinking water bottles that was first separated, washed and shredded. The particles thus derived were then shredded once again, using a propeller crusher in order to control granular limit with crushing. Moreover, they present irregular shape and rough surface texture in order to facilitate matrix-particles adhesion (**Figure 1**). **Figure 2** showed the X-ray diffraction analysis of PET particles and indicated the presence of a backbone form of the polymer which generates sharp peaks at a high angle range $\sim 10^\circ - 35^\circ$. The main mechanical and thermal properties of the plastic used in this study are presented in **Table 3**. Particle size distributions analysis (**Figure 3**) reveals the sand to be particularly coarse (*Fineness modules* = 3.66) and that the upper granular limit value of PET aggregates is 5 mm. After preliminary tests, polymer particles of size lower than 1 mm were used in this study. Absolute density of PET particles (1.35 g/cm^3) is approximately 2.5 times smaller than that of cement

Table 1. Cement chemical composition.

| Oxide analysis (%) | | | | | |
|--------------------------------|-------|--------------------------------|-------|-----------------|------|
| Loss on ignition | 2.08 | Fe ₂ O ₃ | 4.57 | SO ₃ | 1.85 |
| SiO ₂ | 21.83 | CaO | 63.42 | CaO free | 0.25 |
| Al ₂ O ₃ | 6.01 | MgO | 0.22 | | |

Table 2. Physical properties of cement.

| Physical properties | |
|--|------|
| Setting time (min) | |
| Initial | 120 |
| Final | 200 |
| Blaine surface area (cm ² /g) | 2977 |
| Absolute density (g/cm ³) | 3.09 |
| Compressive strength (MPa) 28 days | 32.5 |

Table 3. Physical properties of the PET plastic used.

| Physical properties | |
|-----------------------------------|-----|
| Tensile strength at break (MPa) | 70 |
| Elongation at break (%) | 70 |
| Flexural modulus (rigidity) (MPa) | 2.0 |
| Tensile modulus (GPa) | 2.9 |
| Melting point (°C) | 260 |
| Water absorption (%) | 0 |

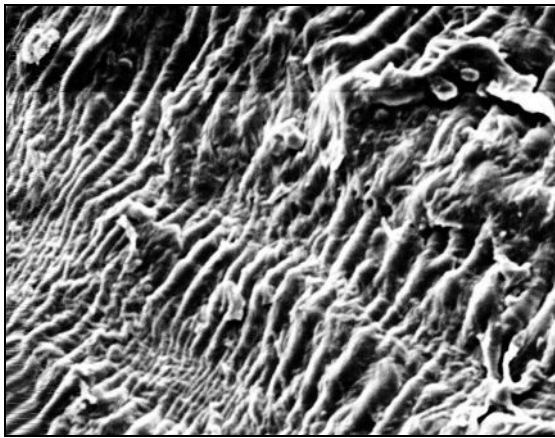


Figure 1. Scanning electron micrographs of PET particles, (magnification, $\times 1200$).

(3.09 g/cm^3). This low density will allow the lightening of PET-mortar composite.

2.2. Composite Mixing Conditions

The mortar manufactured with PET particles was first optimized on the basis of mechanical criteria and then constitutes the reference composite. The composites containing PET particles were produced in accordance with the results of the previous work [35]. A mass ratio of 3 between sand (S) and the cement (C) has been respected. Various mass percentages of cement (2.5%, 5.0% and 7.5%) were substituted by the same weight of granulated plastic waste (**Table 4**). The water to binder

ratio was kept constant at 0.5. The physical properties of the pastes of mortars were determined in accordance with EN 19-3 [36].

The PET particles and cement were first dry-mixed at 140 rpm during 1 min in a standard mixing machine (EN 196-1 [37]) to reach a homogeneous mixture. Then sand was added and the mixing continues during 1 min at low speed. Next, water was gradually added at 140 rpm during 1 min and after the whole is mixed during 1 min with 285 rpm. After pouring fresh material into the molds, samples were stored in both a hygrometrically-controlled and temperature-controlled room (98% relative humidity and $20^\circ\text{C} \pm 2^\circ\text{C}$) for 24 h. After removal from the moulds, at 24 h of age, mortar specimens were immersed in water saturated with lime at $20^\circ\text{C} \pm 3^\circ\text{C}$ until the age of testing. Test results from the **Table 4** of the hydraulic transport properties, sorptivity-value, revealed that the addition of PET particles tends to restrict water propagation in the cement matrix and reduces water absorption of the composite. This may be due both to the capability of PET to repel water (non-sorptive nature, water absorption % = 0, **Table 3**) and to the increase of air-entrainment, as manifested by closed empty pores, which are not accessible to water. This phenomenon serves to reduce the volume accessible to water and hence capillary porosity. The decrease in water absorption is also attributed to a reduction in the porosity near particle/matrix interfacial zone, due to the high bonding between PET additive and cement paste [35]. So, the decrease of the sorptivity-value is favorable to the durability of the specimen structures.

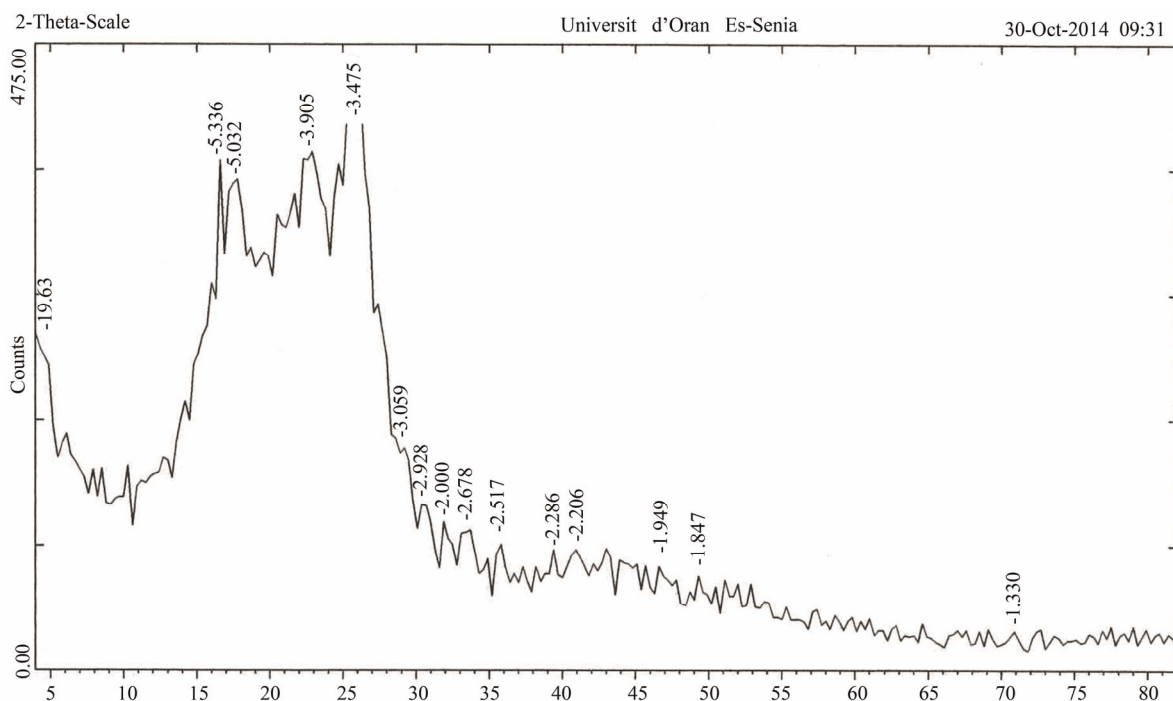
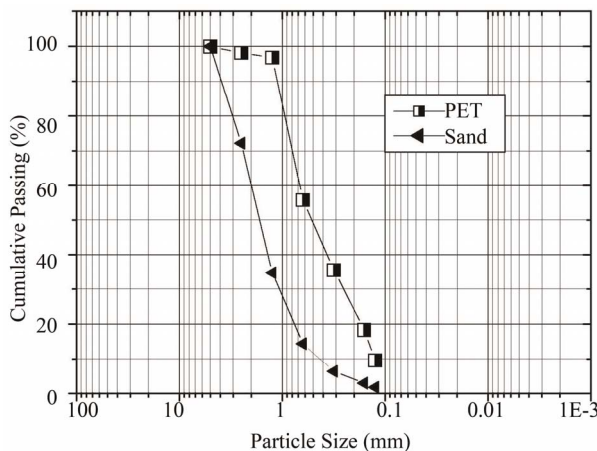
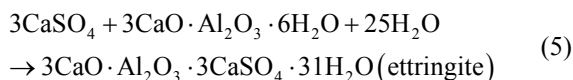
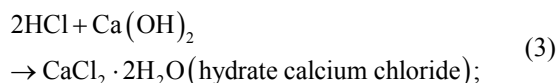


Figure 2. X-ray diffraction pattern of the PET particles.



Hence, **Figure 4** presents the results of compressive strength loss *CSL%* of the mixes at 56 days in different hydrochloric acid concentration (0.5%, 1% and 1.5%) solutions. The results indicate that the resistance of acidic attack of the composites (PET7.5) was increased with an increase in PET content. At day-56, the *CSL%* of PET7.5 was reduced by 68%, 41%, 10.7% for the 0.5%, 1% and 1.5% of HCl acid solutions, respectively, when compared to that of PET0.

The H_2SO_4 solutions lead to the formation of less water-soluble gypsum $CaSO_4$, 0.241g/100ml of H_2O at $20^\circ C$, and ettringite on the surface in contact with the cementing matrix. With CH_3COOH acid, there is a formation of the hydrate calcium acetate $Ca(CH_3COO)_2$, 52.0g/100ml of H_2O . While, the chemicals formed as the products of reaction between hydrochloric acid and hydrated cement phases are some soluble salts, mostly with calcium chloride $CaCl_2$ (dihydrate) that is very water-soluble: 46.08g/100ml of H_2O , which are subsequently leached out, and some insoluble salts along with amorphous hydrogels (iron hydroxide) which remain in the corroded layer. These chemical reactions are shown in Equations (3)-(5). These results are in agreement with those reported by elsewhere [45-47].



Additionally, these results are confirmed by the change of surface samples before and after immersion in the HCl

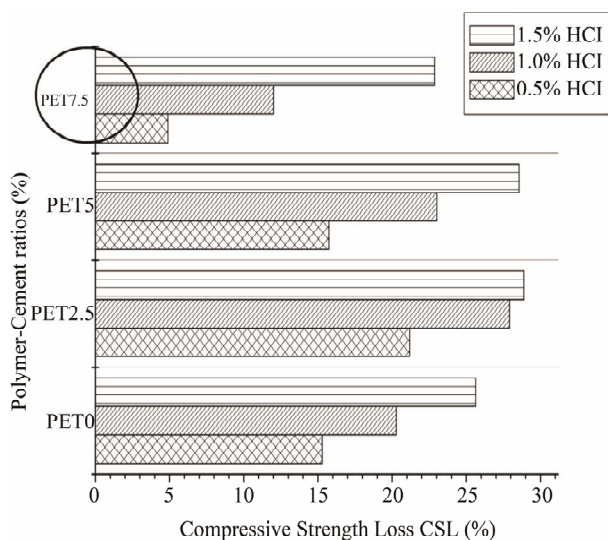
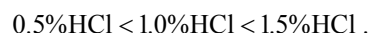


Figure 4. Compressive strength loss of specimens under HCl acid solutions exposure.

aggressive solutions as depicted in **Figure 5**. These mortars kept their rectangular forms more or less, but their dimensions decreased considerably from 0.5%, 1% to 1.5%. Hydrochloric acid attack is a typical acidic corrosion which can be characterized by the formation of layer structure [47]; its can be divided to three main zones: undamaged zone, hydroxide mixture zone or brown ring, and attacked zone. By hydroxide mixture zone, there is a layer formed by undissolved salts seen as a dark brown ring.

The chemical resistance of materials is more or less affected by the concentration and the nature of acids in the order with the most aggressive as given below:



The increase in the resistance to hydrochloric attack of the composites is attributed to the impervious PET granules blocking the passage of the aggressive solutions and the reduction of the sorptivity of PET-mortar composites (**Tables 3 and 4**). Furthermore, the decrease in porosity due to the incorporation of PET in modified mortars [48] contributes to reduce the absorption of acidic solution accompanied by a reduction of loss in weight. These results are in agreement with those reported by Benosman *et al.* [46]. Additionally, different teams of researchers [49-51] reported that the incorporation of organic additions (polymers) increases chemical resistance in aggressive media.

3.1.2. X-Ray Diffraction (XRD) Analysis

Figure 6 presents the XRD analysis of composite PET0, as an example, before and after attack by different hydrochloric acid concentration (0.5%, 1% and 1.5%) solu



Figure 5. Deterioration of specimens after 56 days of immersion; (1) Tap water, (2) 0.5%, (3) 1%, (4) 1.5% HCl acids (From the left to right, respectively).

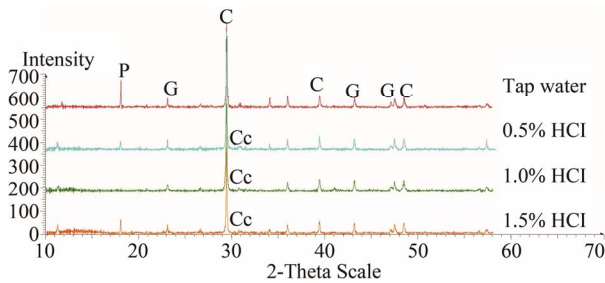


Figure 6. X-ray diffraction pattern of the specimens under HCl acids exposure. P: portlandite $\text{Ca}(\text{OH})_2$, C: calcite, G: gypsum, Cc: $\text{CaCl}_2 \cdot 2\text{H}_2\text{O}$ (hydrated calcium chloride).

tions. The stacking of the various spectra (initial state, after 0.5% attack, after 1% attack and after 1.5% attack) confirms the appearance of a trace of calcium chloride (CaCl_2) on the specimens exposed to hydrochloric acid. The low quantity of calcium chloride found is due to its high solubility in water (46.08g/100ml of H_2O). Washing of each specimen after the immersion period leaves its surface nearly free from this salt. Additionally, the portlandite $\text{Ca}(\text{OH})_2$ was decomposed by different acids concentration following the chemical reaction (Equation (3)).

3.1.3. FT-IR Analyses

Table 5 illustrates the positions and intensities of infrared absorption bands and **Figure 7** shows the FT-IR patterns of specimens exposed to: Tap water, 0.5%, 1% and

1.5% HCl acids solution. The FT-IR spectra of the composite hydrated up to 56 days and cured in water are presented in **Figure 7** and **Table 5**. The major changes of the FT-IR spectra in the hydrated cement pastes are: Calcium hydroxide bands ($\sim 3635 \text{ cm}^{-1}$) and also for the free OH groups, combined and adsorbed water of CSH, AFm and AFt phases ($\sim 3480 \text{ cm}^{-1}$), molecular water ($3440 - 3446$ and $1614 - 1621 \text{ cm}^{-1}$), carbonate phases (~ 1425 , 870.03 and 708 cm^{-1}). The broad band at $\sim 1020 - 1016 \text{ cm}^{-1}$ arises from C-S-H vibrations, in agreement with those reported by Martinez-Ramirez [52].

As the same for the X-ray diffraction, the FT-IR analysis of composite after attack by different acids (**Table 5**, **Figure 7**) confirms the appearance of a trace of calcium chloride (CaCl_2) on the specimens exposed to various HCl acids. The low quantity of calcium chloride found is due to its high solubility in water.

Therefore, in **Table 5** and **Figure 7** no absorption bands corresponding to calcium hydroxide were detected in all of specimens exposed to acidic solutions, which is in agreement with XRD analysis. The $\text{Ca}(\text{OH})_2$ was consumed by different HCl acids following the chemical reaction (Equation (3)).

3.1.4. DTA-TGA/dTG Analyses

The simultaneously traced DTA-TGA curves of PET0 composite before and after HCl acids attack (0.5%, 1% and 1.5%) are presented in **Figures 8-11**.

Table 5. Fourier-transform infrared table of composite before and after attack by different HCl acids, in KBr pellet.

| Positions and Intensities of Infrared Absorption Bands (FT-IR) | | | | |
|--|---|---|-----------|-------------------------|
| (cm^{-1}) | Group | Compounds | Tap water | HCl (0.5%, 1% and 1.5%) |
| $\sim 3000 - 3700$ | H_2O , OH, hydrogen bonds | Gypsum, CSH | +++ | + |
| ~ 3636 (Fine) | H_2O , OH, hydrogen bonds | portlandite | +++ | --- |
| $3450 - 3485$ | H_2O , OH | AFm, AFt | ++ | + |
| $1614 - 1621$ | H_2O , ν O-H | H_2O | + | + |
| $1425 - 1433$ | ν C-O | CaCO_3 (Calcite) | + | + |
| $869 - 874$ | ν C-O | CaCO_3 (Calcite) | + | + |
| $705 - 710.6$ | ν C-O | CaCO_3 (Calcite) | + | + |
| $\sim 1015 - 1029$ | ν Si-O | CSH vibrations | + | + |
| $\sim 470 - 524; 535$ | ν Ca-Cl | $\text{CaCl}_2 \cdot 2\text{H}_2\text{O}$ | 0 | +++ |
| ~ 2970 | ν C-O (harmonic bands) | CaCO_3 (Calcite) | + | + |
| $2865 - 2871$ | ν C-O (harmonic bands) | CaCO_3 (Calcite) | + | + |
| $2512 - 2518$ | ν C-O (harmonic bands) | CaCO_3 (Calcite) | + | + |
| ~ 1799 | ν C-O (harmonic bands) | CaCO_3 (Calcite) | + | + |

AFt: $\text{C}(\text{A}, \text{F}) \cdot 3\text{CaSO}_4 \cdot 32\text{H}_2\text{O}$; AFm: $\text{C}_3\text{A} \cdot 3\text{CaSO}_4 \cdot 12\text{H}_2\text{O}$.

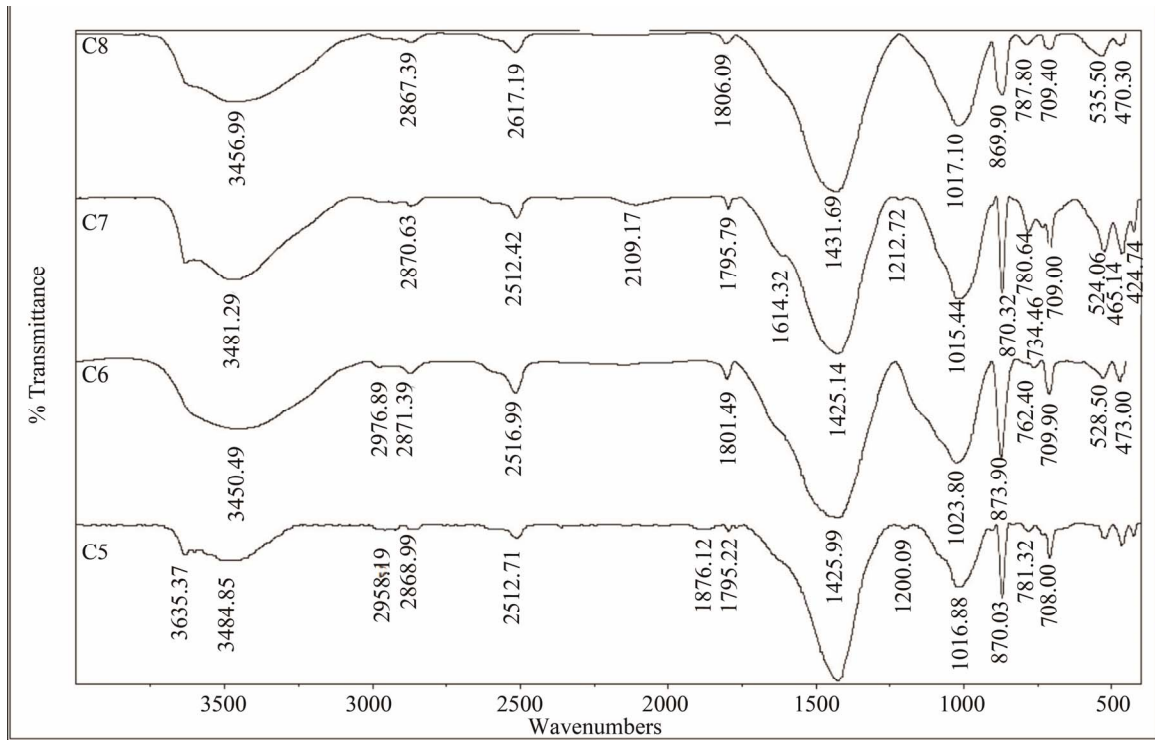


Figure 7. FT-IR spectra of the specimens under HCl acid exposure, (C5: Tap water, C6: 0.5%, C7: 1%, C8: 1.5%).

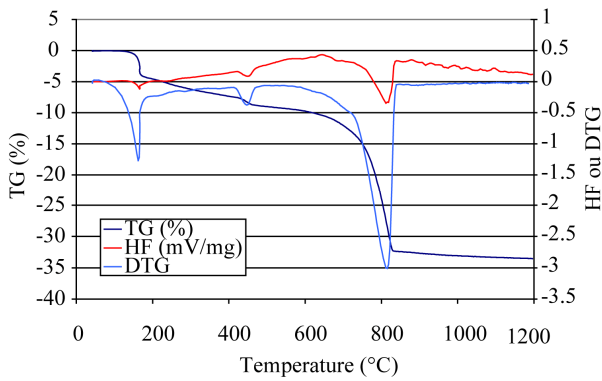


Figure 8. DTA/TG curves at 20 K/min of composite PET0 in tap water exposure.

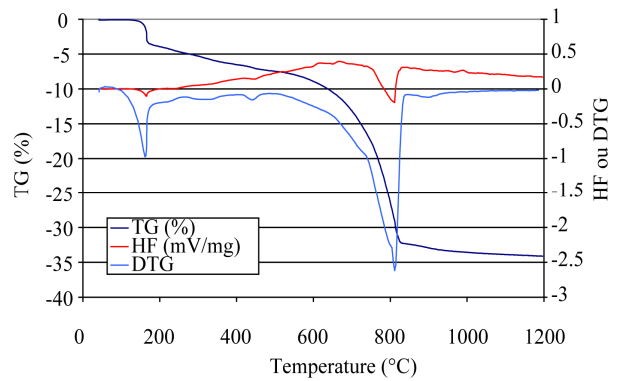


Figure 10. DTA/TG curves at 20 K/min of composite PET0 under 1.0% hydrochloric acid exposure.

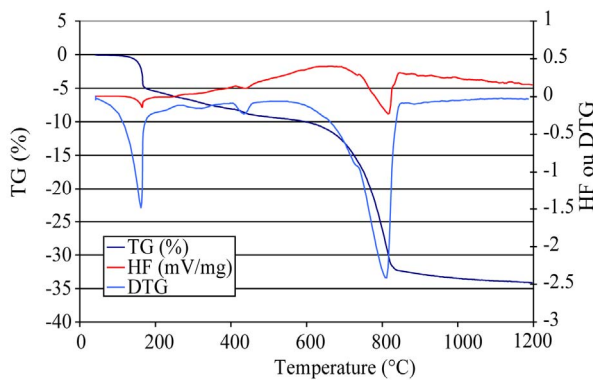


Figure 9. DTA/TG curves at 20 K/min of composite PET0 under 0.5% hydrochloric acid exposure.

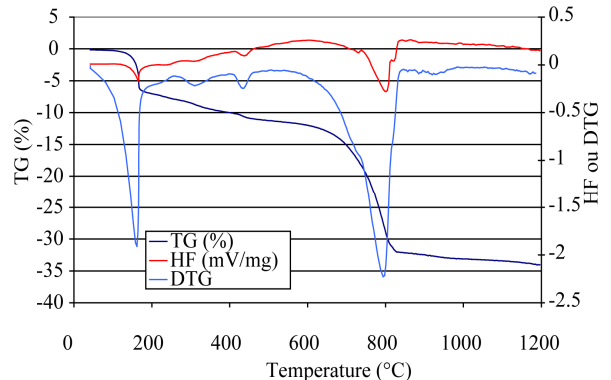


Figure 11. DTA/TG curves at 20 K/min of composite PET0 under 1.5% hydrochloric acid exposure.

Figure 8 shows the DTA/TG curves of mortar without polymer PET0 in the tap water. It can be seen that DTA-TG/dTG curves for this mortar consist of four zones:

~100°C - 150°C: dehydration of pore water (CSH, ettringite),

~225°C - 230°C: dehydration of calcium aluminates hydrates,

~450°C - 550°C: dehydroxylation of calcium hydroxide,

~700°C - 850°C: decarbonation of CaCO₃.

Figures 9-11 show DTA-TG/dTG curves of PET0. As it is shown, the curves can be divided into four major parts, according to different reactions:

~100°C - 145°C: dehydration of pore water,

~225°C - 230°C: dehydration of calcium aluminates hydrates,

~440°C - 540°C: the reduction of the intensity of the peak corresponding to dehydroxylation of portlandite, which indicates that, with exposure all the Ca(OH)₂ that was formed reacted with the HCl acid solutions (Equation (3)).

~700°C - 850°C: decarbonation of CaCO₃.

All the weight loss data are expressed as a function of the ignited weight of the sample, as suggested by Taylor [53]. The calcium hydroxide content was determined from the following equation:

$$CH(\%) = WL_{CH}(\%) \times \frac{MW_{CH}}{MW_H} \quad (6)$$

where $CH(\%)$ is the content of Ca(OH)₂ (in weight basis), $WL_{CH}(\%)$ is the weight loss occurred during the dehydration of calcium hydroxide (in weight basis), MW_{CH} is the molar weight of calcium hydroxide and MW_H is the molar weight of water.

When one attacks the PET0 composite by the hydrochloric acid at 0.5%, 1% and 1.5%, there is a diminution of the calcium hydroxide (CH) content, as can be seen in **Figure 12**. Because when the concentration of acid increases, there is less formation of portlandite Ca(OH)₂, which is mainly consumed following the chemical reaction (Equation (3)). This confirms our previous results.

3.1.4. Scanning Electron Microscope (SEM)

Observations

In case of HCl attack, the damaged of PET0 composite was selected as an example to observe the microstructure of deterioration and the SEM images are shown in **Figure 13**. No portlandite crystal exists in the acid attacked composite. It is clear that exposure to solution of hydrochloric acid generates pores and micro-cracks in the mortar specimens. So, The SEM and ATD-TG/dTG analyses corroborate some of the results discussed above.

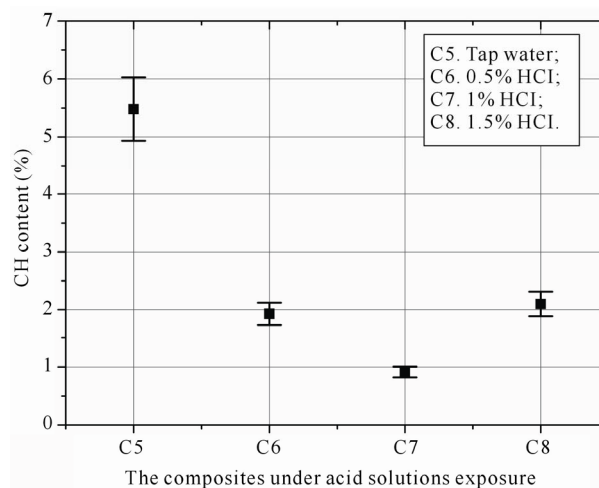


Figure 12. Effect of HCl acids concentration on the calcium hydroxide content (CH).

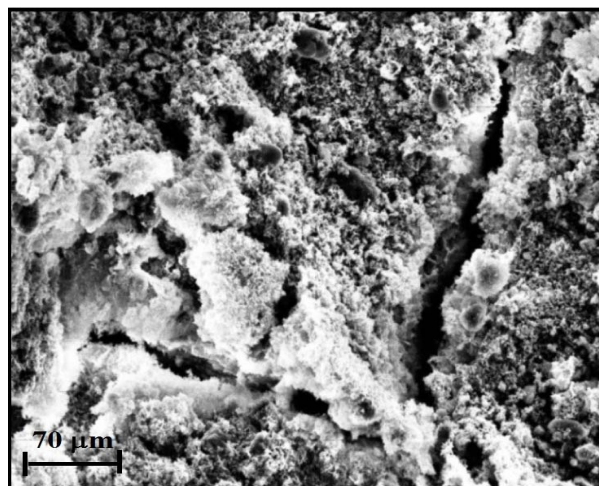
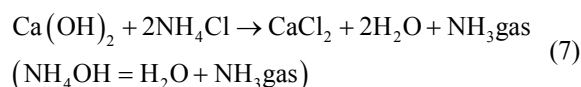


Figure 13. SEM images obtained for the external porous texture of PET0 sample after being attacked by the 1% hydrochloric acid solution ($\times 600$).

3.2. Ammonium Chloride NH₄Cl Attack

Figures 14 and 15 show the evolution of the degraded thickness of composite immersed in a solution of ammonium chloride 10%, represented as a function of the polymer-cement ratios. Loss of mass followed the same trend. At 480 days, significant differences were obtained: compared to PET0, the depth of attack was 16.2%, 26.2% and 34.8% lower for PET2.5, PET5 and PET7.5, respectively.

Ammonium salts are generally more destructive than salts of other bases [54]. So, ammonium chloride is very aggressive and reacts following an exchange mechanism $2NH_4^+ \rightarrow Ca^{2+}$ given by the reaction:



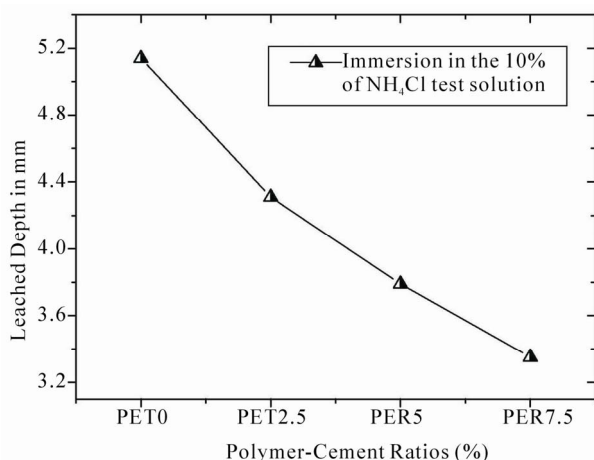


Figure 14. Depth of attack due to the leaching of composite immersed in 10% ammonium chloride.

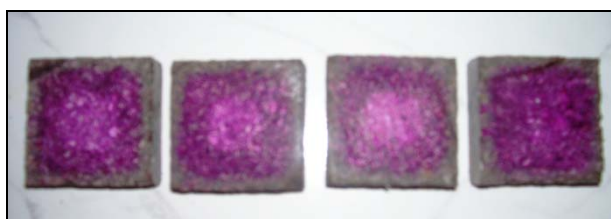


Figure 15. Depth of reduced lixiviation of the composites PET0, PET2.5, PET5 and PET7.5 (from the left to right) indicated by the phenolphthalein solution.

This reaction leads to the formation of a highly soluble calcium chloride (46.08 g/100ml of H₂O) and a release of ammonia. The resulting reduction of the pH impedes the reaction to reach a state of equilibrium. The consequence is progressive leaching of portlandite and C-S-H, thus leading to a decrease of the mechanical properties of mortar. The reaction with aluminates leads to the formation of a hydrated calcium chloride aluminate 3CaO·Al₂O₃·CaCl₂·10H₂O [55].

As for most of the other tests, the composites were the modified mortar most resistant to this acid attack (pH = 5.6). This might be due to impervious PET granules blocking the passage of the aggressive solutions and the reduction of the sorptivity of modified mortar (Tables 3 and 4). Furthermore, the decrease in porosity due to the incorporation of PET in composite [48] contributes to reduce the absorption of acidic solution accompanied by a reduction of loss in weight. However, no pertinent data were found concerning the effect of PET against ammonium chloride attack.

3.3. Ammonium Sulfate (NH₄)₂SO₄ and H₂SO₄ Attacks

Figure 16 shows the percentage change with respect to time in the weight of cubes immersed in sulfuric acid and

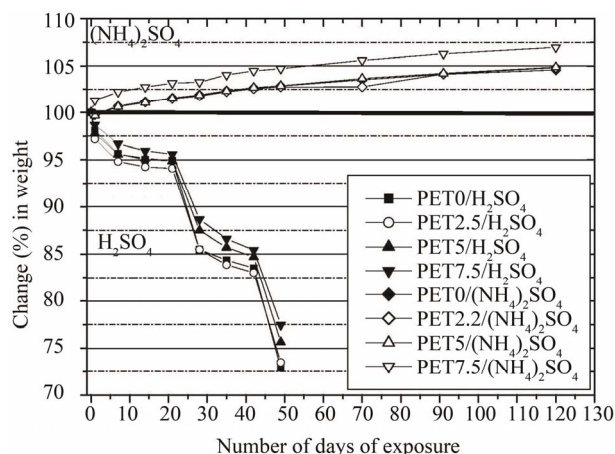


Figure 16. Change (%) in weight with time under H₂SO₄ acid and (NH₄)₂SO₄ solutions.

ammonium-sulfate. It can be seen in the same figure that there is an increase in weight of cubes immersed in ammonium sulfate for the period of experimentation. The augmentation in weight after 120 days of immersion was 4.5%, 4.8%, 4.86% and 6.9% for PET0, PET2.5, PET5 and PET7.5 respectively. However, in the cubes immersed in sulfuric acid it can be noted that the reduction in weight has occurred. So, the rate of reduction in weight was less in PET5 and PET7.5. The mass loss for PET7.5 is lower than the corresponding PET0 mortar by 5% (Figure 16).

The increase in the weight of composites immersed in sulfatic solutions can be explained by the formation of expansive products. In the presence of water, the sulfates ions react with calcium aluminates hydrate (C₃A) and/or the components of the calcium hydroxide of hardened cement paste to form calcium sulfoaluminate hydrate commonly called "ettringite" [56] and calcium sulfate (gypsum). However, it is important to recognize that the end products of the various reactions, if they occur so as to damage the mortar or concrete, result in different types of damage [57]. Mehta [58] reported that the 5% (NH₄)₂SO₄ solution proved to be more aggressive than 1% H₂SO₄; it appears that ammonium salts are able to decompose the calcium hydrate, which is the principal solid phase in hydrated portland cement pastes. In consequence, different preventive measures are required.

Compressive strength losses CSL% of PET-composites samples after curing in water for 28 days and exposed in 10% of ammonium-sulfate solution for 860 days and in 5% of sulfuric acid for 56 days are presented in Figure 17. It can be seen that the modified mortar samples containing polyethylene terephthalate have better behaviour in ammonium-sulfate solution. The results indicate that the resistance to (NH₄)₂SO₄ solution of the composites was increased with an increase in PET content. At day-860, the CSL% of PET2.5, PET5 and

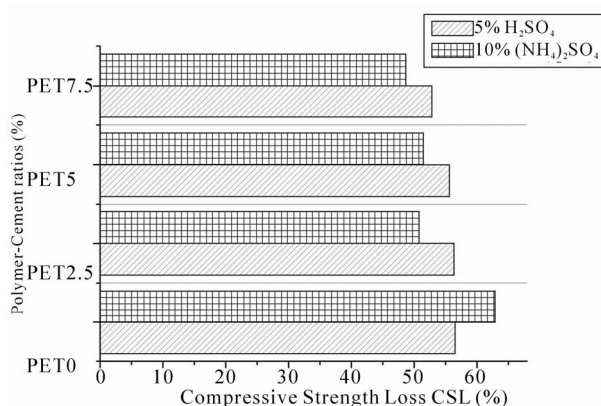


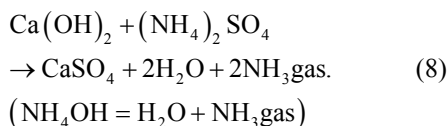
Figure 17. Compressive strength loss of specimens under H₂SO₄ acid and (NH₄)₂SO₄ solutions exposure.

PET7.5 were reduced by 19.2%, 18.2% and 22.6%, respectively, when compared to that of PET0. In addition, at 56 days, there is a CSL% diminution around 7% for PET7.5 compared to an unmodified one in sulfuric acid solution (Figure 17).

Therefore, the increase in the resistance to ammonium-sulfate of the composites is attributed to the impervious PET granules blocking the passage of the aggressive solution and the reduction of the sorptivity of polymer-mortar (Tables 3 and 4). Consequently, the decrease in porosity due to the incorporation of PET in modified mortars [48] contributes to reduce the absorption of sulfates solution. These results are in agreement with those reported elsewhere [46]. The same explanation was also done for the PET7.5 in the sulfuric acid. Additionally, different teams of researchers [49-51] reported that the incorporation of organic additions (polymers) increases chemical resistance in aggressive media.

It can be concluded that adding PET to blended portland cement makes this cement become more resistant to the ammonium-sulfate aggressive environment. It is evident that the resistance of cement to sulfate aggression is also related to the content of C₃A in them [27]. However, no pertinent data were found concerning the effect of PET against ammonium sulfate attack.

Ammonium sulfate is very aggressive and reacts following an exchange mechanism $2\text{NH}_4^+ \rightarrow \text{Ca}^{2+}$ given by the reaction:



This reaction leads to the formation of less water-soluble gypsum CaSO₄, 0.241 g/100 ml of H₂O and a release of ammonia. Calcium sulfate formed as described above can subsequently react with C₃A, usually via the formation of mono-sulfoaluminate, to form ettringite (Equation (5)). In addition, attack of hydrated Portland

cement by H₂SO₄ acid is two-fold. The first one is by acid attack or hydrogen ions and the second is by the sulfuric ions. Two salts are formed: namely calcium sulfate and ettringite (Equations (4) and (5)). These are destructive salts and the pressure produced during their formation causes mortar to crack and disintegrate.

Comparing the exposure of mortars to sulfuric acid and ammonium sulfate, it is immediately apparent that the mechanisms involved are quite different. So, Rendell *et al.* [59] reported that sulfuric acid causes a heavy deposition of gypsum that acts as a protective layer; this surface protection is verified by the unchanged hardness beyond a depth of 2 mm, however, it is noted that gypsum is deposited at depths of up to 2 mm in fissures and voids. In this case the mechanism of attack is caused by the production of the expansive gypsum, this expansive effect being responsible for the progressive opening of the material structure by dislocation of surface material. It was noted from the SEM and microanalysis [59], that there is a filling of fissures and pores with gypsum, this deposition will have the effect of producing an internal blocking of the pore structure. It is, therefore, proposed that the surface deposit of gypsum, if not removed by scour forms a protective layer thus limiting the attack rate.

The samples exposed to ammonium sulfate experienced a significant deterioration in material hardness up to a depth of 5 mm [59]. However, from the microanalysis it was noted that there was little sulfur evident behind the surface; the major site of gypsum formation being at the surface. It is proposed that the mechanism of deterioration in this case is one of dissolution of Ca²⁺ from the mortar. Leaching of Ca²⁺ is principally the result of the dissolution of portlandite; this action causes an opening of the pore structure of the mortar and is, therefore, responsible for the reduction in mechanical strength and ultimate loss in durability [59].

3.3.1. Visual Inspection

Additionally, in case of H₂SO₄ and (NH₄)₂SO₄ attacks, the damaged of PET0 composite was selected as an example to observe the macrostructure of deterioration. So, these results are confirmed by the change of surface samples before and after immersion in the aggressive solutions. A visual inspection of specimens as shown in Figure 18 revealed the deterioration of the samples, particularly for the mortars immersed in sulfuric acid. These mortars kept their cubic forms more or less, but their dimensions decreased considerably.

Photos of specimens stored in the ammonium sulfate solution for 120 and 860 days are presented in Figure 18. The samples stored for 120 days under ammonium sulfate exposure showed the first signs of deterioration, while the specimens stored in tap water did not show any



(a)



(b)



(c)



(d)

Figure 18. Specimens cubes (50 mL) exposed to: (a) Tap water, (b) H_2SO_4 (56 days), (c) $(\text{NH}_4)_2\text{SO}_4$ (120 days), (d) $(\text{NH}_4)_2\text{SO}_4$ (860 days).

clear evidence of attack. The discussion below concerns the samples stored in $(\text{NH}_4)_2\text{SO}_4$ solution. In all cases, the first sign of attack was the deterioration of the corners, followed by cracking along the edges. Progressively, expansion and spalling took place on the surface of the specimens.

After 860 days of immersion in a solution of 10% $(\text{NH}_4)_2\text{SO}_4$, all 4 surfaces of the specimens developed a white cover that was friable and started to peel off, leaving the aggregates uncovered and reducing the connec-

tivity of the paste. Thus, the extent of surface deterioration after 860 days of exposure had a tendency to decrease with the increased replacement level of the PET wastes.

Polymer-mortar composites modified with PET waste can be advantageous for special applications where the main request is not for mechanical properties, such as in the production of sound barriers and cement blocks for lightweight concrete walls. Also, these composites are often used as low-cost materials for preventing chemical

attacks or repairing various reinforced concrete structures damaged by chloride-induced corrosion [21,22], as well as in structures exposed to aggressive environments where high resistance to ammonium-sulfate/-chloride, acid, basic and chloride solutions is required.

3.3.2. X-Ray Diffraction (XRD) Analysis

Figure 19 presents the XRD analysis of PET0 composite, as an example, before and after attack by different sulfuric acid and ammonium sulfate solutions. The common factor for all hydrated samples is the presence of portlandite Ca(OH)_2 and ettringite

$\text{Ca}_6\text{Al}_2(\text{SO}_4)_3(\text{OH})_{12} \cdot 26\text{H}_2\text{O}$. Unlike these samples from the sulfuric acid and ammonium sulfate solution which are marked by considerable quantities of gypsum ($\text{CaSO}_4 \cdot 2\text{H}_2\text{O}$), the samples which were in water contain minimal quantity of gypsum. As gypsum existed in the initial material in both cases, it is evident that during the process of hydration it served, together with other components, to form ettringite, for water cured samples.

Opposite to this, the quantity of formed ettringite is small and similar in all the samples exposed to ammonium sulfate, which points out to the assumption that mostly sulfate ions only from gypsum present in the initial samples participated in the forming of ettringite. These results are in agreement with those reported by Miletić *et al.* [27]. We also noted that portlandite Ca(OH)_2 was completely decomposed by different acid and sulfate solutions following the chemical reactions 4, 5 and 8.

3.3.3. FT-IR Analyses

Table 6 illustrates the positions and intensities of infrared absorption bands and **Figures 20** and **21** show the FT-IR patterns of specimens exposed to: Tap water, H_2SO_4 , and $(\text{NH}_4)_2\text{SO}_4$. The FT-IR spectra of the composite hydrated up to 28 days and cured in water are presented in **Figure 20** and **Table 6**. The major changes of

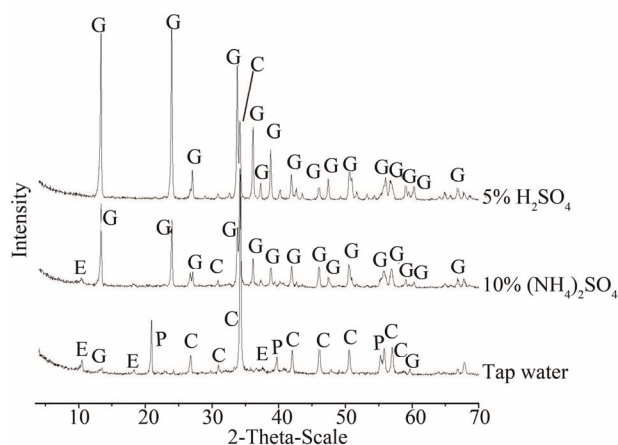


Figure 19. X-ray diffraction pattern of the specimens under H_2SO_4 acid and $(\text{NH}_4)_2\text{SO}_4$ solutions exposure. P: portlandite Ca(OH)_2 ; E: ettringite; C: calcite; G: gypsum.

the FT-IR spectra in the hydrated cement pastes are: Calcium hydroxide bands ($\sim 3637\text{ cm}^{-1}$) and also for the free OH groups, combined and adsorbed water of CSH, AFm and AFt phases (3452 cm^{-1}), molecular water ($3425\text{ - }3445$ and $1641\text{ - }1660\text{ cm}^{-1}$), carbonate phases ($\sim 1428, 874.5$ and 712.5 cm^{-1}). The broad band at $\sim 990\text{ - }1020\text{ cm}^{-1}$ arises from C-S-H vibrations, in agreement with those reported by Martinez-Ramirez [52].

As the same for the X-ray diffraction, the FT-IR analysis of composites after attack by acid and sulfate solutions (**Table 6**, **Figures 20** and **21**) confirms the appearance of a large quantity of gypsum ($\text{CaSO}_4 \cdot 2\text{H}_2\text{O}$) on the specimens exposed to H_2SO_4 and $(\text{NH}_4)_2\text{SO}_4$ and a small quantity of ettringite on the specimens exposed to ammonium sulfate.

Therefore, in **Table 6** and **Figures 20** and **21** no absorption bands corresponding to calcium hydroxide were detected in all of specimens exposed to acidic and ammonium sulfate solutions, which is in agreement with XRD analysis. The Ca(OH)_2 was consumed by aggressive solutions following the chemical reactions 4, 5 and 8.

To obtain further evidence to corroborate these observations from XRD and FT-IR, further investigation was made using SEM, DSC and TG/dTG analyses.

3.3.4. Scanning Electron Microscope (SEM) Observations

The composite of PET0 exposed to $(\text{NH}_4)_2\text{SO}_4$ solutions was selected as an example to observe the microstructure of deterioration products, and the SEM images are shown in **Figure 22**. No portlandite Ca(OH)_2 crystal existed in the sulfate-attacked unmodified mortar, and many club-shaped or needle-like crystals were embedded irregularly in the pulpy material with a very open microstructure. **Figure 22(a)** shows a large number of needle-like ettringite crystals, smaller than $2\mu\text{m}$ in diameter and $10\text{ - }11\mu\text{m}$ in length, and the existence of different morphologies of the C-S-H gel in the specimen covering the mortar surface before sulfation. In the pores or surface cracks, there were many club-shaped gypsum crystals, which had much larger sizes (smaller than $100\text{ - }200\mu\text{m}$ in diameter and $300\text{ - }500\mu\text{m}$ in length) than the ettringite, as shown in **Figure 22(b)**. The formation of both ettringite and gypsum led to the cracking, spalling, and decomposition of the unmodified mortar exposed to a sulfate environment (**Figure 22(c)**). The combination of XRD, FT-IR and SEM led to the positive identification of the deterioration products' formation.

The surface that was exposed to sulfuric acid had a nature that was quite different. The scanning electron microscopy (SEM) observations were also carried out to identify the products formed by attack of PET0 in the

Table 6. Fourier-transform infrared table of composite before and after attack by different acid and sulfate solutions, in KBr pellet.

| Positions and Intensities of Infrared Absorption Bands (FT-IR) | | | | | |
|--|--------------------------------------|-----------------------------|-----------|--------------------------------|---|
| (cm ⁻¹) | Group | Compounds | Tap water | H ₂ SO ₄ | (NH ₄) ₂ SO ₄ |
| ~3000 - 3600 | H ₂ O, OH, hydrogen bonds | Gypsum, CSH | ++ | + | + |
| ~3637.09 | H ₂ O, OH, hydrogen bonds | portlandite | ++ | 0 | 0 |
| 3424 - 3452 | H ₂ O, OH | AFm, AFt | + | + | ++ |
| 1623 - 1660 | H ₂ O, OH | H ₂ O | + | + | + |
| 1428 - 1439 | ν C-O | CaCO ₃ (Calcite) | + | + | + |
| 873 - 875 | ν C-O | CaCO ₃ (Calcite) | + | + | + |
| 710 - 713 | ν C-O | CaCO ₃ (Calcite) | + | + | + |
| ~990 - 1020 | ν Si-O | CSH vibrations | + | +(w,sh) | + |
| ~1130 - 1142 | ν S-O | Gypsum | ~ | +++ | +++ |
| ~604.5 - 672 | δ S-O | Gypsum | ~ | +++ | +++ |
| ~3408 - 3546 | ν O-H | water (Gypsum) | ~ | +++ | +++ |
| ~1622 - 1687 | δ O-H | water (Gypsum) | ~ | +++ | +++ |
| ~1105 - 1110 | δ S-O (sulfates) | Ettringite | + | 0 | ~ |
| ~602 - 608 | δ S-O (sulfates) | Ettringite | + | 0 | ~ |
| 2982 | ν C-O (harmonic bands) | CaCO ₃ (Calcite) | + | + | + |
| 2872 | ν C-O (harmonic bands) | CaCO ₃ (Calcite) | + | + | + |
| ~2515 | ν C-O (harmonic bands) | CaCO ₃ (Calcite) | + | + | + |
| ~1798 | ν C-O (harmonic bands) | CaCO ₃ (Calcite) | + | + | + |

w: weak, sh: shoulder, AFt: C(A,F)·3CaSO₄·32H₂O; AFm: C₃A·3CaSO₄·12H₂O.

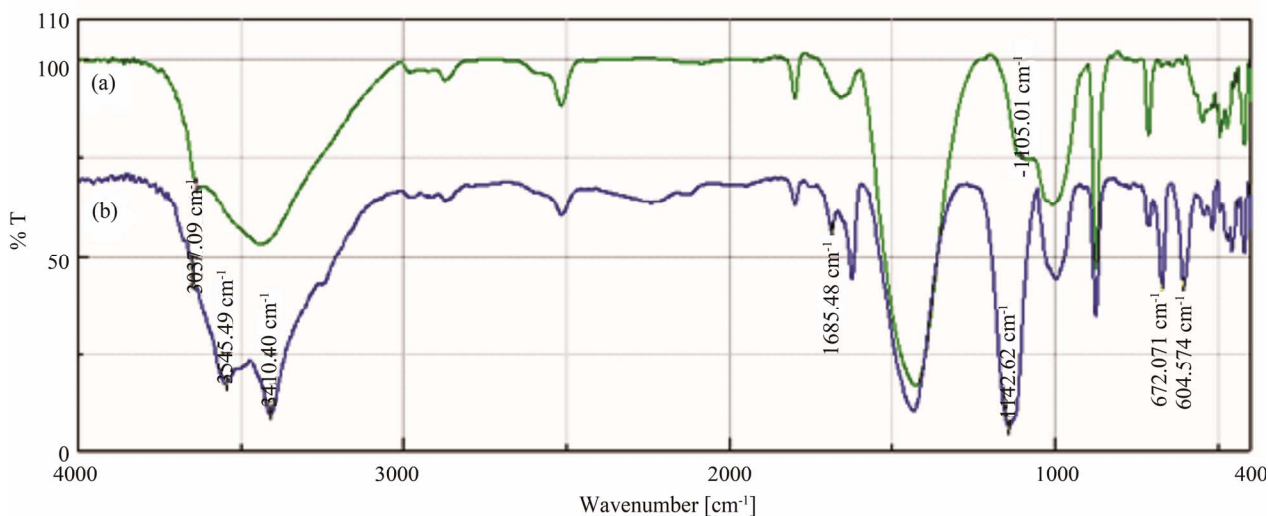


Figure 20. FT-IR spectra of the specimens under (a) Tap water and (b) (NH₄)₂SO₄ solution exposure.

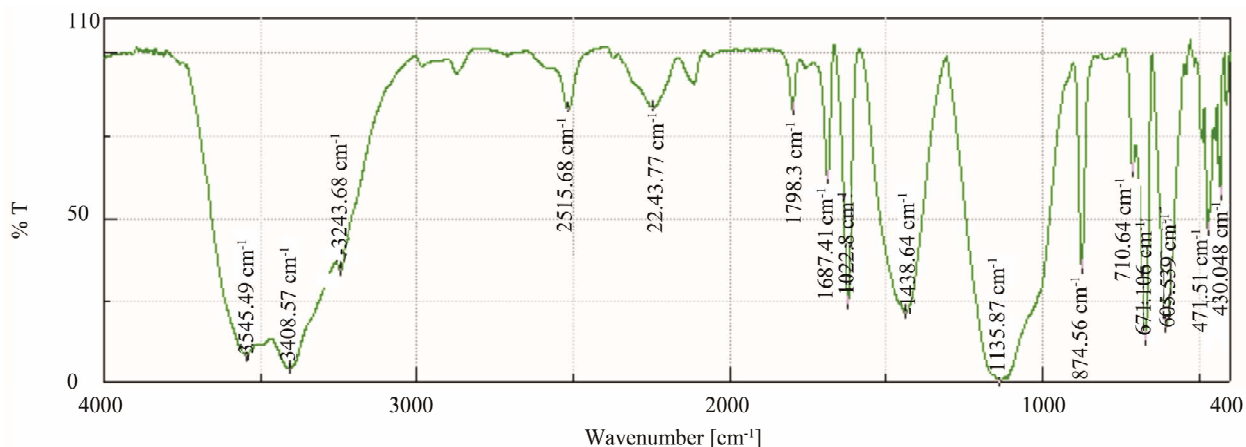


Figure 21. FT-IR spectra of the specimens under sulfuric acid exposure.

sulfuric acid solutions and the results are exhibited in **Figure 23**. In addition, **Figure 23** taken around a crack on the surface of the core sample shows deposition of a large number of needle-like crystals (gypsum), smaller than 36 - 40 μm in diameter and 300 - 500 μm in length, covering the mortar surface. In the pores or surface cracks, there are many club-shaped gypsum crystals as shown in **Figure 23**. The formation of gypsum leads to the cracking, spalling, and decomposition of mortar exposed to sulfuric acid environment. The SEM images obtained by SEM corroborate some of the results discussed above.

Consequently, our results are in agreement with those reported by Rendell *et al.* [59] which showed that when cement mortar is exposed to sulfuric acid a dense layer of gypsum is formed; this is capable of retarding the deterioration process by acting as a surface sealing layer. Gypsum also exists in pores and fissures in the surface zone, indicating that the attack is due to expansive crystallisation. In ammonium sulfate the surface deposit of gypsum is sparse and the damage to the concrete occurs to a greater depth. The lack of sulfur found in the surface zone indicates that the mechanism of deterioration is due to the dissolution of Ca^{2+} .

3.3.5. DSC and TG/dTG Analyses

The DSC and TG/dTG curves of PET0 composite before and after $(\text{NH}_4)_2\text{SO}_4$ solution and H_2SO_4 acid attack are presented in **Figures 24-26**.

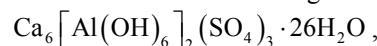
Figure 24 shows the DSC curves of unmodified mortar PET0 in the tap water. It can be seen that DSC curves for this mortar consist of three zones:

- ~90°C - 115°C: dehydration of pore water (CSH, ettringite),
- ~145°C - 157°C: dehydration of calcium sulphate (Gypsum),
- ~450°C - 500°C: dehydroxylation of calcium hydroxide, portlandite.

Figure 25 presents the DSC trace of PET0 after ammonium sulphate attack; it displays four endothermic peaks, according to different reactions:

~100°C - 145°C: dehydration of pore water,

~115°C - 120°C: ettringite



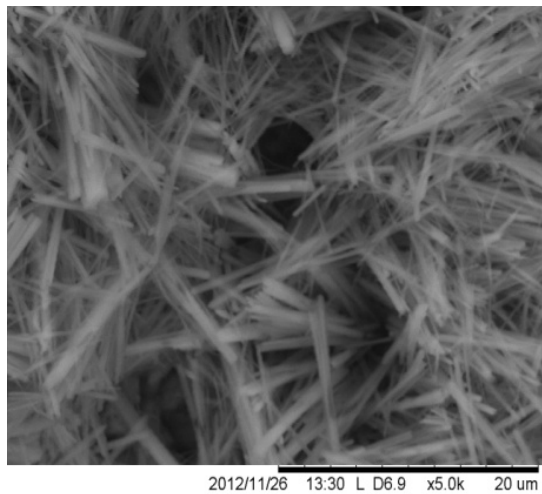
~140°C - 145°C: the intensity of the peak due to calcium sulphate $\text{CaSO}_4 \cdot 2\text{H}_2\text{O}$ is greater. So, gypsum was the dominant reaction product (Equation (8)) while the ettringite appeared as a trace element in the composite.

~440°C - 510°C: In PET0 composite there was no endothermic peak at 462°C, which indicates that, with exposure all the $\text{Ca}(\text{OH})_2$ that was formed reacted with the ammonium sulphate solution.

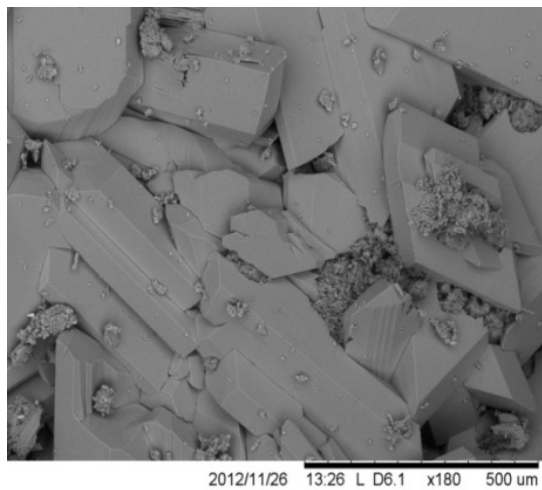
Figure 26 presents the TG/dTG trace for the surface part of the sample obtained from the PET0 composite stored in 5% sulphuric acid solution; it displays three endothermic peaks at 157 (High intensity), 210 and 850°C - 900°C, indicating gypsum, calcium monocarboaluminate hydrated and decarbonation of the calcite CaCO_3 . Also, TG/dTG analysis showed no endothermic peak at 462°C, which indicates that, with exposure all the $\text{Ca}(\text{OH})_2$ that was formed reacted with the sulphuric acid solution (Equation (4)).

Hence, the DSC, TG/dTG curves obtained by DSC and TG/dTG analyses corroborate some of the results discussed above.

It should be pointed out that, in practice, the durability of composites exposed to the chemical solutions investigated in this study should be much better than indicated by the test data given here. First, because the chemical solutions of high concentrations used in the test are not commonly encountered in food and most other industries. Second, the composite specimens in the test were fully submerged, whereas in the industrial practice the structural element such as floor is usually exposed to attack



(a)



(b)



(c)

Figure 22. SEM photos of the PET0 composite after exposure to 10% $(\text{NH}_4)_2\text{SO}_4$ solution for 860 days; (a) Needle-like ettringite crystals, (b) Club-shaped gypsum crystals and (c) deteriorate mortar.

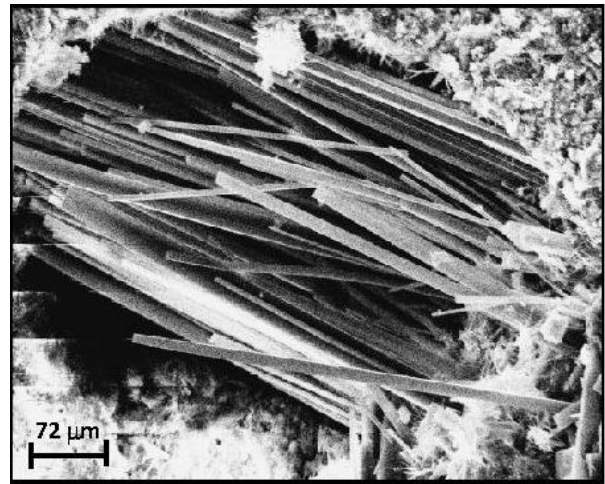


Figure 23. SEM photos of the PET0 composite after exposure to 5% H_2SO_4 solution ($\times 600$) for 56 days; needle-like crystals (gypsum) in the pore.

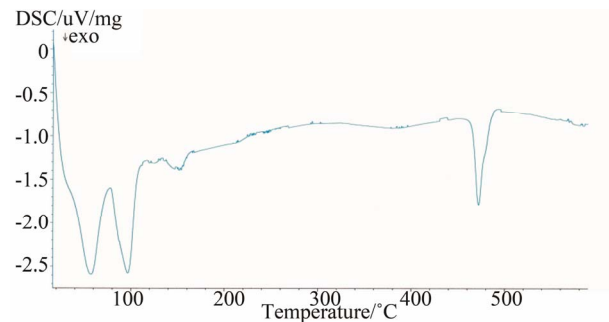


Figure 24. DSC curves at 10 K/min of composite PET0 in tap water exposure.

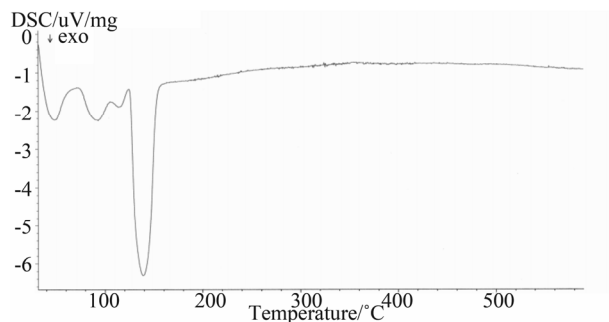


Figure 25. DSC curves at 10 K/min of composite PET0 in $(\text{NH}_4)_2\text{SO}_4$ solution exposure.

from one side only. Third, the immersion solutions were kept in state of constant motion, and were frequently replaced which fresh brushing of the specimens once every week; this removed the reaction products and almost continuously forced new material to come into contact with aggressive solution.

4. Conclusions

The influence of the PET particles on PET-modified

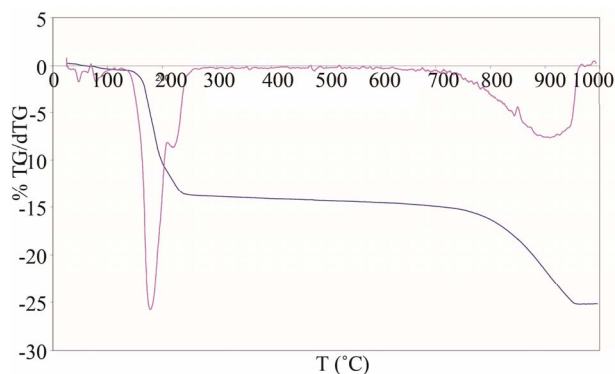


Figure 26. TG/dTG curves at 10 K/min of composite PET0 in H_2SO_4 acid exposure.

mortar composites sorptivity, mechanical strength and the chemical properties under hydrochloric acid, ammonium-chloride, ammonium-sulfate and sulfuric acid attack solutions were determined. The results of testing the attack by aggressive solutions allow the following conclusions:

1) Test results of the hydraulic transport properties revealed that the addition of PET particles tends to restrict water propagation in the cement matrix and reduces water absorption of the composite. The decrease of the sorptivity-value is favorable to the durability of the specimen structures.

2) The results of specific indicators for ammonium chloride, ammonium-sulfate and acid attacks showed that an increase in the PET content led to better resistance of the composite. This may be due to the reduced volume of large-sized pores and the improved resistance to the absorption of aggressive solutions with the addition of PET in the cement pastes, because of the impervious PET particles blocking the passage of the aggressive ions. In addition, to the reduction in the porosity near particle/matrix interfacial zone, due to the high bonding between PET additive and cement paste.

3) Among composite mixes in the HCl acid attacks, PET7.5 mixes perform better than other mixes. The chemical resistance characteristics of materials are affected by the concentration and by the nature of acids following the order: $0.5\%HCl < 1.0\%HCl < 1.5\%HCl$. Additionally, from the simultaneously traced DTA/TG curves there is a diminution of the calcium hydroxide (CH) content, because of the formation of calcium chloride which has a high solubility in water.

4) On the basis of the XRD, FT-IR and DSC analyses of the changes in the phase composition, it can be concluded that the main product of the ammonium-sulfate corrosion of cement is gypsum, accompanied by ettringite. The common factor for all hydrated samples is the presence of portlandite $Ca(OH)_2$ and ettringite $Ca_6Al_2(SO_4)_3(OH)_{12} \cdot 26H_2O$. The samples exposed to

the ammonium-sulfate solution show considerable quantities of gypsum $CaSO_4 \cdot 2H_2O$. The quantity of ettringite formed is small and very similar in all the samples, which points out to the assumption that mostly sulfate ions only from gypsum present in the initial samples participated.

5) The SEM results show that the presence of sulfur ions is virtually existent in the matrix of composites exposed to ammonium sulfate. It is proposed that the reduction in mechanical hardness can be attributed to a migration of Ca^{2+} from the outer layers of the unmodified mortar.

6) The mechanism of attack in the case of composite exposed to sulfuric acid is principally a surface phenomenon, the expansive action of the gypsum acting to dislocate aggregate and to increase micro cracking at the surface. It is evident from the SEM that there is a filling of pores and micro fissures with gypsum (Tg/dTG). In the absence of erosion this layer has a surface blocking ability.

The utilization of the PET waste particles as a binder instead of cement in the manufacture of PET-mortar composites and as a sustainable building materials in the construction industry help to preserve natural resources and maintain the ecological balance and also to prevent or repair various reinforced concrete structures.

5. Acknowledgements

The authors acknowledge the financial support from the Ministry of Higher Education and Scientific Research of Algeria, under the grants CNEPRU J0405520120005. The authors greatly appreciated the technical support from the Laboratory of LUSAC EA 2607, University of Caen Basse-Normandie, Cherbourg Octeville (French) and also would like to thank Mr M. T. Gouasmi and the graduate students, Mrs. A. Herizi and A. Kerour for their help.

REFERENCES

- [1] S. Miletić, M. Ilić, J. Ranogajec, R. Marinović-Nedudin, and M. Djurić, "Portland Ash Cement Degradation in Ammonium-Sulfate Solution," *Cement and Concrete Research*, Vol. 28, No. 5, 1998, pp. 713-725. [doi:10.1016/S0008-8846\(98\)00023-4](https://doi.org/10.1016/S0008-8846(98)00023-4)
- [2] Y. Ohama, "Polymer Based Admixtures," *Cement and Concrete Composite*, Vol. 20, No. 2-3, 1998, pp. 189-212. [doi:10.1016/S0958-9465\(97\)00065-6](https://doi.org/10.1016/S0958-9465(97)00065-6)
- [3] Y. Ohama, "Hand Book of Polymer-Modified Concrete and Mortars, Properties and Process Technology," Noyes Publications, Park Ridge, 1995, p. 236.
- [4] D. W. Fowler, "Polymers in Concrete: A Vision for the 21st Century," *Cement and Concrete Composites*, Vol. 21, No. 5-6, 1999, pp. 449-452. [doi:10.1016/S0958-9465\(99\)00032-3](https://doi.org/10.1016/S0958-9465(99)00032-3)

- [5] N. Saikia and J. de Brito, "Use of Plastic Waste as Aggregate in Cement Mortar and Concrete Preparation: A review," *Construction and Building Materials*, Vol. 34, 2012, pp. 385-401.
[doi:10.1016/j.conbuildmat.2012.02.066](https://doi.org/10.1016/j.conbuildmat.2012.02.066)
- [6] R. Siddique, J. Khatib and I. Kaur, "Use of Recycled Plastic in Concrete: A review," *Waste Management*, Vol. 28, No. 10, 2008, pp. 1835-1852.
[doi:10.1016/j.wasman.2007.09.011](https://doi.org/10.1016/j.wasman.2007.09.011)
- [7] K. F. Portella, A. Joukoski, R. Franck and R. Derksen, "Reciclagem Secundária de Rejeitos de Porcelanas Elétricas em Estruturas de Concreto: Determinação do Desempenho sob Envelhecimento Acelerado," *Cerâmica*, Vol. 52, No. 323, 2006, pp. 155-167.
[doi:10.1590/S0366-69132006000300008](https://doi.org/10.1590/S0366-69132006000300008)
- [8] I. Guerra, I. Vivar, B. Llamas, A. Juan and J. Moran, "Eco-efficient Concretes: The Effects of Using Recycled Ceramic Material from Sanitary Installations on The Mechanical Properties of Concrete," *Waste Management*, Vol. 29, No. 2, 2009, pp. 643-646.
[doi:10.1016/j.wasman.2008.06.018](https://doi.org/10.1016/j.wasman.2008.06.018)
- [9] Z. Z. Ismail and E. A. Al-Hashmi, "Use of Waste Plastic in Concrete Mixture as Aggregate Replacement," *Waste Management*, Vol. 28, No. 11, 2008, pp. 2041-2047.
- [10] S. C. Angulo, C. Ulsen, V. M. John, H. Kahn and M. A. Cincotto, "Chemical-Mineralogical Characterization of C&D Waste Recycled Aggregates from São Paulo, Brazil," *Waste Management*, Vol. 29, No. 2, 2009, pp. 721-730.
- [11] C. Hoppen, K. F. Portella, A. Joukoski, E. M. Trindade and C. V. Andreóli, "Uso de Lodo de Estação de Tratamento de Agua Centrifugado, em Matriz de Concreto de Cimento Portland para Reduzir o Impacto Ambiental," *Química Nova*, Vol. 29, No. 1, 2006, pp. 79-84.
- [12] K. S. Rebeiz, "Time-Temperature Properties of Polymer Concrete Using Recycled PET," *Cement and Concrete Composites*, Vol. 17, No. 2, 1995, pp. 119-124.
[doi:10.1016/0958-9465\(94\)00004-1](https://doi.org/10.1016/0958-9465(94)00004-1)
- [13] YW. Choi, DJ. Moon, YJ. Kim, M. Lachemi, "Characteristics of Mortar and Concrete Containing Fine Aggregate Manufactured from Recycled Waste Polyethylene Terephthalate Bottles," *Construction and Building Materials*, Vol. 23, No. 8, pp. 2829-2835.
[doi:10.1016/j.conbuildmat.2009.02.036](https://doi.org/10.1016/j.conbuildmat.2009.02.036)
- [14] Y. W. Choi, D. J. Moon, J. S. Chung and S. K. Cho, "Effects of PET Waste Bottles Aggregate on the Properties of Concrete," *Cement and Concrete Research*, Vol. 35, No. 4, 2005, pp. 776-781.
[doi:10.1016/j.cemconres.2004.05.014](https://doi.org/10.1016/j.cemconres.2004.05.014)
- [15] B. JO, G. Tae and C. Kim, "Uniaxial Creep Behavior and Prediction of Recycled-PET Polymer Concrete," *Construction Building Materials*, Vol. 21, 2007, pp. 1552-1559. [doi:10.1016/j.conbuildmat.2005.10.003](https://doi.org/10.1016/j.conbuildmat.2005.10.003)
- [16] T. Ochi, S. Okubo and K. Fukui, "Development of Recycled PET Fiber and Its Application as Concrete Reinforcing Fiber," *Cement and Concrete Composites*, Vol. 29, No. 6, 2007, pp. 448-455.
[doi:10.1016/j.cemconcomp.2007.02.002](https://doi.org/10.1016/j.cemconcomp.2007.02.002)
- [17] A. Khaloo, M. Dehestani and P. Rahmatabadi, "Mechanical Properties of Concrete Containing a High Volume of Tire-Rubber Particles," *Waste Management*, Vol. 28, No. 12, 2008, pp. 2472-2482.
[doi:10.1016/j.wasman.2008.01.015](https://doi.org/10.1016/j.wasman.2008.01.015)
- [18] J. C. A. Galvão, K. F. Portella, A. Joukoski, R. Mendes and E. S. Ferreira, "Use of waste polymers in concrete for repair of dam hydraulic surfaces," *Construction and Building Materials*, Vol. 25, No. 2, 2011, pp. 1049-1055.
[doi:10.1016/j.conbuildmat.2010.06.073](https://doi.org/10.1016/j.conbuildmat.2010.06.073)
- [19] R. Wang and C. Meyer, "Performance of Cement Mortar Made With Recycled High Impact Polystyrene," *Cement & Concrete Composites*, Vol. 34, No. 9, 2012, pp. 975-981. [doi:10.1016/j.cemconcomp.2012.06.014](https://doi.org/10.1016/j.cemconcomp.2012.06.014)
- [20] V. Corinaldesi, A. Mazzoli, G. Moriconi, "Mechanical Behaviour and Thermal Conductivity of Mortars Containing Waste Rubber Particles," *Materials and Design*, Vol. 32, No. 3, 2011, pp. 1646-1650.
[doi:10.1016/j.matdes.2010.10.013](https://doi.org/10.1016/j.matdes.2010.10.013)
- [21] A. S. Benosman, H. Taibi, M. Mouli, M. Belbachir and Y. Senhadji, "Diffusion of Chloride Ions in Polymer-Mortar Composites (PET)," *Journal of Applied Polymer Science*, Vol. 110, No. 3, 2008, pp. 1600-1605.
[doi:10.1002/app.28587](https://doi.org/10.1002/app.28587)
- [22] A. S. Benosman, H. Taibi, M. Belbachir, I. Bahlouli, M. Mouli, Y. Senhadji and D. Houivet, "Resistance of Polymer (PET)-Mortar Composites to Chloride Penetration," *Proceedings of 7th Asian Symposium on Polymers in Concrete ASPIC 2012*, Istanbul, 3-5 October 2012, pp. 387-395.
- [23] M. T. Gouasmi, A. S. Benosman, H. Taibi, M. Belbachir and Y. Senhadji, "Elaboration and Characterization of Polymer-Siliceous Sand Composites," *2nd French Meeting on Insulating Materials RFMI-2*, Oran, 17-19 December 2012.
- [24] M. T. Gouasmi, "Effects of Polyethylene Terephthalate Lightweight Aggregates on the Properties of Mortar," *Magister Thesis*, University of Oran, Oran, 2013, p. 153.
- [25] "ECO PET," 2007.
http://www.ecopet.eu/Domino_english/ecopet.htm
- [26] The Korea Institute of Resources Recycling, "The Korean Institute of Resources Recycling, Recycling Handbook," The Korea Institute of Resources Recycling, Seoul, 1999.
- [27] S. Miletić, M. Ilić, S. Otović, R. Folić and Y. Ivanov, "Phase Composition Changes Due to Ammonium-Sulphate: Attack on Portland and Portland Fly Ash Cements," *Construction and Building Materials*, Vol. 13, No. 3, 1999, pp. 117-127.
[doi:10.1016/S0950-0618\(99\)00017-3](https://doi.org/10.1016/S0950-0618(99)00017-3)
- [28] H. F. W. Taylor, "Crystal Structure of Some Double Hydroxide Minerals," *Mineralogical Magazine*, Vol. 39, No. 304, 1973, pp. 247-256.
[doi:10.1180/minmag.1973.039.304.01](https://doi.org/10.1180/minmag.1973.039.304.01)
- [29] S. Miletić, M. Ilić, J. Ranogajec and M. Djurić, "Sulphate Corrosion of Portland Cement and Portland Cement Mixed With Fly Ash and Slag as a Function of its Composition," *Proceedings of XVI Symposium on Nordic Concrete Research*, Helsinki, 1996, pp. 339-340.
- [30] S. Miletić and M. Ilić, "Sulphate Corrosion of Portland

- Cement with Various Mineral Compositions, *Proceedings of the 13th International Corrosion Congress*, Melbourne, 1996, pp. 1-7.
- [31] V. Zivica and A. Bajza, "Acidic Attack of Cement Based Materials—A Review. Part 1. Principle of Acidic Attack," *Construction and Building Materials*, Vol. 15, No. 8, 2001, pp. 331-340. [doi:10.1016/S0950-0618\(01\)00012-5](https://doi.org/10.1016/S0950-0618(01)00012-5)
- [32] P. K. Mehta, "Concrete, Properties and Materials," Prentice-Hall, Upper Saddle River, 1986.
- [33] W. H. Gutt and W. H. Harrison, "Chemical Resistance of Concrete," *Concrete*, Vol. 11, No. 5, 1997, pp. 35-37.
- [34] V. Zivica and A. Bajza, "Acidic Attack of Cement-Based Materials—A Review Part 2. Factors of Rate of Acidic Attack and Protective Measures," *Construction and Building Materials*, Vol. 16, 2002, pp. 215-222. [doi:10.1016/S0950-0618\(02\)00011-9](https://doi.org/10.1016/S0950-0618(02)00011-9)
- [35] A. S. Benosman, H. Taïbi, M. Belbachir, I. Bahlouli, M. Mouli, Y. Senhadji and D. Houivet, "Mineralogical Study of Polymer-Mortar Composites with PET Polymer by Means of Spectroscopic Analyses," *Materials Sciences and Applications*, Vol. 3, No. 3, 2012, pp. 139-150. [doi:10.4236/msa.2012.33022](https://doi.org/10.4236/msa.2012.33022)
- [36] EN 196-3, "Methods of Testing Cement—Part 3: Determination of Setting Time and Soundness," Comité Européen de Normalisation, Brussels, 1995.
- [37] EN 196-1, "Methods of testing cement—Part 1: Determination of Strength," Comité Européen de Normalisation, Brussels, 1995.
- [38] ASTM C 267-97, "Standard Test Methods for Chemical Resistance of Mortars, Grouts, and Monolithic Surfacing and Polymer Concretes," American Society for Testing and Materials (ASTM) International, West Conshohocken, 1997.
- [39] ASTM C1012-04, "Standard Test Method for Length Change of Hydraulic-Cement Mortars Exposed to a Sulfate Solution," American Society for Testing and Materials (ASTM) International, West Conshohocken, 2004.
- [40] C. Carde, G. Escadeillas and R. François, "Use of Ammonium Nitrate Solution to Simulate and Accelerate the Leaching of Cement Pastes due To Deionized Water," *Magazine Concrete Research*, Vol. 181, No. 49, 1997, pp. 295-301. [doi:10.1680/mac.1997.49.181.295](https://doi.org/10.1680/mac.1997.49.181.295)
- [41] N. Kaid, M. Cyr, S. Julien and H. Khelafi, "Durability of Concrete Containing a Natural Pozzolan as Defined by a Performance-Based Approach," *Construction and Building Materials*, Vol. 23, No. 12, 2009, pp. 3457-3467. [doi:10.1016/j.conbuildmat.2009.08.002](https://doi.org/10.1016/j.conbuildmat.2009.08.002)
- [42] Z. T. Chang, X. J. Song, R. Munn, M. Marosszeky, "Using Limestone Aggregates and Different Cements for Enhancing Resistance of Concrete to Sulphuric Acid Attack," *Cement and Concrete Research*, Vol. 35, No. 8, 2005, pp. 1486-1494. [doi:10.1016/j.cemconres.2005.03.006](https://doi.org/10.1016/j.cemconres.2005.03.006)
- [43] S. Goyal, M. Kumar, D. S. Sidhu and B. Bhattacharjee, "Resistance of Mineral Admixture Concrete to Acid Attack," *Journal of Advanced Concrete Technology*, Vol. 7, No. 2, 2009, pp. 273-283. [doi:10.3151/jact.7.273](https://doi.org/10.3151/jact.7.273)
- [44] H. Siad, H. A. Mesbah, H. Khelafi, S. Kamali-Bernard and M. Mouli, "Effect Of Mineral Admixture on Resistance to Sulphuric and Hydrochloric Acid Attacks in Self-Compacting Concrete," *Canadian Journal of Civil Engineering*, Vol. 37, No. 3, 2010, pp. 441-449. [doi:10.1139/L09-157](https://doi.org/10.1139/L09-157)
- [45] D. Achoura, Ch. Lanos, R. Jauberthie and B. Redjel, "Influence d'une Substitution Partielle du Ciment par du Laitier de Hauts Fourneaux Sur la Résistance des Mortiers en Milieu Acide," *Journal de Physique IV France, EDP Sciences*, Vol. 118, No. 1, 2004, pp. 159-164. [doi:10.1051/jp4:2004118019](https://doi.org/10.1051/jp4:2004118019)
- [46] A. S. Benosman, M. Mouli, H. Taïbi, M. Belbachir and Y. Senhadji, "Resistance of Polymer (PET)-Mortar Composites to Aggressive Solutions," *International Journal of Engineering Research in Africa*, Vol. 5, No. 1, 2011, pp. 1-15. [doi:10.4028/www.scientific.net/JERA.5.1](https://doi.org/10.4028/www.scientific.net/JERA.5.1)
- [47] A. Allahverdi and F. Škvára, "Acidic Corrosion of Hydrated Cement Based Materials—Part 1. Mechanism of the Phenomenon," *Ceramics-Silikáty*, Vol. 44, No. 3, 2000, pp. 114-120.
- [48] A. S. Benosman, "Mechanical Performance and Durability of Cementitious Materials Modified by Adding Polymer (PET)," Ph.D. Thesis, University of Oran, Algeria, 2010.
- [49] J.-A. Rossignolo, M.-V.C. Agnesini, "Durability of Polymer-Modified Lightweight Aggregate Concrete," *Cement and Concrete Composites*, Vol. 26, No. 4, 2004, pp. 375-380. [doi:10.1016/S0958-9465\(03\)00022-2](https://doi.org/10.1016/S0958-9465(03)00022-2)
- [50] J. Monteny, N. De Belie, E. Vincke, W. Verstraete and L. Taerwe, "Chemical and Microbiological Tests to Simulate Sulfuric Acid Corrosion of Polymer-Modified Concrete," *Cement and Concrete Research*, Vol. 31, No. 9, 2001, pp. 1359-1365.
- [51] S. Chandra and L. Berntsson, "Lightweight Aggregate Concrete-Science, Technology, and Applications," *William Andrew Publishing/Noyes*, Chapter 8, 2002, pp. 231-240.
- [52] S. Martínez-Ramírez, "Influence of SO₂ Deposition on Cement Mortar Hydration," *Cement and Concrete Research*, Vol. 29, No. 1, 1999, pp. 107-111. [doi:10.1016/S0008-8846\(98\)00183-5](https://doi.org/10.1016/S0008-8846(98)00183-5)
- [53] H. F. W. Taylor, "Studies on the Chemistry and Microstructures of Cement Pastes," *Proceedings of the British Ceramic Society*, Vol. 35, 1984, pp. 65-82.
- [54] C. L. Page and M. M. Page, "Durability of Concrete and Cement Composites," Woodhead Publishing, Cambridge England, 2007, p. 404.
- [55] V. Ukraincik, D. Bjecovic and A. Djurekovic, "Concrete corrosion in a nitrogen fertilizer plant," In: P. J. Sere daand and G. G. Litvan, Eds., *Durability of building materials and components*, ASTM, Philadelphia, 1978, pp. 397-409.
- [56] A. Vichot and J.-P. Ollivier, "La durabilité des bétons," Presses de l'École nationale des Ponts et chaussées, ENPC, France, 2008.
- [57] A. M. Neville, "The Confused World of Sulfate Attack on Concrete," *Cement and Concrete Research*, Vol. 34, No.

8, 2004, pp. 1275-1296.

[doi:10.1016/j.cemconres.2004.04.004](https://doi.org/10.1016/j.cemconres.2004.04.004)

- [58] P. K. Mehta, "Studies on Chemical resistance of low water/cement ratio concretes," *Cement and Concrete Research*, Vol. 15, No. 6, 1985, pp. 969-978.

[doi:10.1016/0008-8846\(85\)90087-0](https://doi.org/10.1016/0008-8846(85)90087-0)

- [59] F. Rendell and R. Jauberthie, "The Deterioration of Mortar in Sulphate Environments," *Construction and Building Materials*, Vol. 13, No. 6, 1999, pp. 321-327.
[doi:10.1016/S0950-0618\(99\)00031-8](https://doi.org/10.1016/S0950-0618(99)00031-8)